Article

Immunity

Excessive negative regulation of type I interferon disrupts viral control in individuals with Down syndrome

Graphical abstract

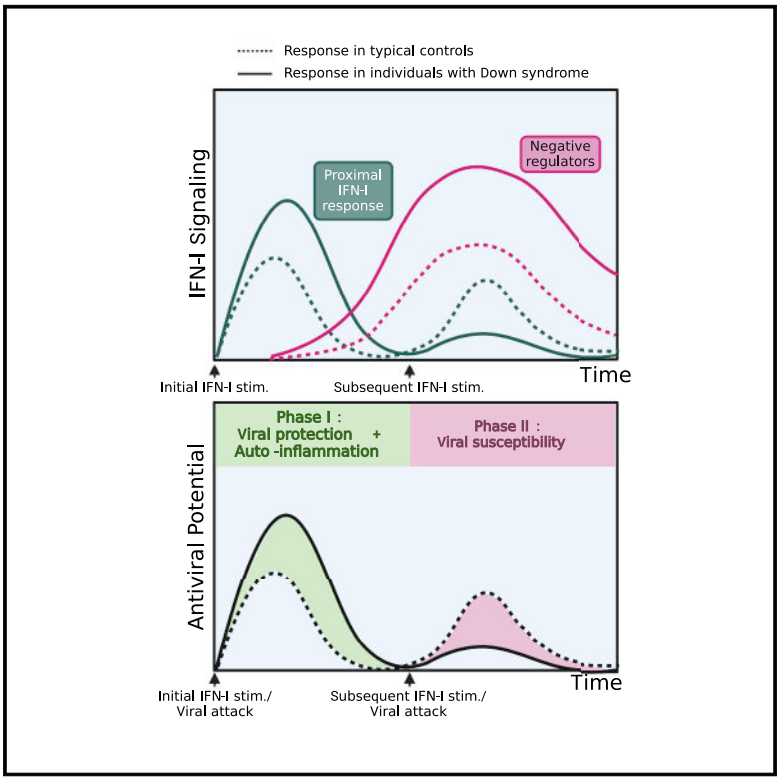

Authors

Louise Malle, Marta Martin-Fernandez, Sofija Buta, Ashley Richardson, Douglas Bush, Dusan Bogunovic

Correspondence

dusan.bogunovic@mssm.edu

In brief

Individuals with Down syndrome have fewer viral infections, but when infected, they suffer from more severe disease. Malle et al. find that triplication of *IFNAR1* and *IFNAR2*, the receptor subunits of the potent antiviral cytokine IFN-I, in DS results in hyperactive IFN-I signaling. The ensuing hyperinduction of IFNAR negative regulators suppresses subsequent IFN-I stimuli and effectively represses further antiviral defenses.

Highlights

- Triplication of *IFNAR1* and *IFNAR2* in DS leads to hyperactive IFN-I response *in vitro*
- Excessive IFN-I signaling triggers negative feedback and ensuing viral susceptibility
- Increased *IFNAR2* expression alone is sufficient to replicate DS IFN-I phenotype
- Monocytes from individuals with DS have basal IFN-I activation and muted IFN-I response

Malle et al., 2022, Immunity *55*, 2074–2084
November 8, 2022
https://doi.org/10.1016/j.immuni.2022.09.007

CellPress

CellPress

Immunity

Article

Excessive negative regulation of type I interferon disrupts viral control in individuals with Down syndrome

Louise Malle,[1,2,3,4,5] Marta Martin-Fernandez,[1,2,3,4,5] Sofija Buta,[1,2,3,4,5] Ashley Richardson,[1,2,3,4,5] Douglas Bush,[2] and Dusan Bogunovic[1,2,3,4,5,6,*]

[1]Center for Inborn Errors of Immunity, Icahn School of Medicine at Mount Sinai, New York, NY, USA
[2]Department of Pediatrics, Icahn School of Medicine at Mount Sinai, New York, NY, USA
[3]Mindich Child Health and Development Institute, Icahn School of Medicine at Mount Sinai, New York, NY, USA
[4]Precision Immunology Institute, Icahn School of Medicine at Mount Sinai, New York, NY, USA
[5]Department of Microbiology, Icahn School of Medicine at Mount Sinai, New York, NY, USA
[6]Lead contact
*Correspondence: dusan.bogunovic@mssm.edu
https://doi.org/10.1016/j.immuni.2022.09.007

SUMMARY

Down syndrome (DS) is typically caused by triplication of chromosome 21. Phenotypically, DS presents with developmental, neurocognitive, and immune features. Epidemiologically, individuals with DS have less frequent viral infection, but when present, these infections lead to more severe disease. The potent antiviral cytokine type I Interferon (IFN-I) receptor subunits IFNAR1 and IFNAR2 are located on chromosome 21. While increased IFNAR1/2 expression initially caused hypersensitivity to IFN-I, it triggered excessive negative feedback. This led to a hypo-response to subsequent IFN-I stimuli and an ensuing viral susceptibility in DS compared to control cells. Upregulation of IFNAR2 expression phenocopied the DS IFN-I dynamics independent of trisomy 21. $CD14^+$ monocytes from individuals with DS exhibited markers of prior IFN-I exposure and had muted responsiveness to *ex vivo* IFN-I stimulation. Our findings unveil oscillations of hyper- and hypo-response to IFN-I in DS, predisposing individuals to both lower incidence of viral disease and increased infection-related morbidity and mortality.

INTRODUCTION

Down syndrome (DS), or trisomy 21, is the most common chromosomal anomaly in the United States, affecting 1 in 700 newborns (Mai et al., 2019). This syndrome affects multiple organ systems, causing a heterogenous clinical presentation that includes intellectual disability, developmental delays, congenital heart and gastrointestinal abnormalities, and Alzheimer's disease in older individuals with DS (Bull, 2020). Recently, it has become clear that abnormal antiviral response is another important feature of DS. A recent study of the largest cohort of individuals with DS to date revealed protection from most infections in DS compared to non-DS controls, including influenza A virus (IAV) (odds ratio [OR]:0.62, $p < 0.0001$), unspecified upper respiratory infections (OR:0.37, $p < 0.0001$), mononucleosis (OR:0.32, $p = 0.0010$), Herpes zoster (OR:0.26, $p < 0.0001$), and intestinal infections (OR:0.50, $p < 0.0001$) (Fitzpatrick et al., 2022). Despite this initial protection, there is extensive evidence that, once infected, patients with DS are more likely to progress to severe disease, including pneumonia (OR: 4.13–6.60), in particular viral pneumonia, acute respiratory distress syndrome, and sepsis (Bruijn et al., 2007; Uppal et al., 2015; Santoro et al., 2021; Fitzpatrick et al., 2022). Increased rates of hospitalization have been documented for IAV, respiratory syncytial virus (RSV), and severe acute respiratory syndrome (SARS) due to coronavirus 2 (SARS-CoV-2) infections (Pérez-Padilla et al., 2010; Mitra et al., 2018; Malle et al., 2020, 2021). Infection-related mortality accounts for 20%–40% of deaths in people with DS, compared to ~4.5% in the general population before the COVID-19 pandemic (Bcheraoui et al., 2018; O'Leary et al., 2018).

While the clinical phenotype of people with DS shows clear signs of immune disturbance, it has yet to be elucidated how a supernumerary chromosome 21 leads to dysregulation of viral defenses. The etiology is likely multi-factorial, given the presence of an extra set of ~200 genes, but delineating the mechanisms at play is essential for improving the care of people with DS. Studies on the adaptive immune system have shown a profound decrease in B cell numbers and altered B cell subsets and also suggest that T cells can be over-activated and exhausted (Verstegen and Kusters, 2020). Evidence of innate immune dysfunction in DS has also started to emerge. Recently, studies have shown that the increased copy number of *IFNAR1* and *IFNAR2*, which encode the two units of the type I interferon receptor (IFNAR), results in overactivation of the

type I interferon (IFN-I) pathway in DS (Sullivan et al., 2016; Kong et al., 2020).

IFN-Is are potent pro-inflammatory cytokines that are essential for fighting against viral infections (Taft and Bogunovic, 2018). To prevent overt inflammation, negative feedback is put in place: IFN-I signaling induces the production of negative regulators (such as USP18) that bind to the receptor, prevent further signaling, and restore homeostasis (François-Newton et al., 2011; Zhang et al., 2015). The hyperresponse to IFN-I previously reported in DS is in line with the lower incidence of most viral infections described epidemiologically. However, an important question remains: why are people with DS more susceptible to infection-related morbidity and mortality? In this study, we interrogate how increased copy number of *IFNAR1* and *IFNAR2* contributes to IFN-I negative regulation, and we examine its effects on viral susceptibility. Our findings add to our understanding of the immune disturbances in DS and help to resolve the clinical paradox of concurrent initial viral protection and increased risk of infection-induced complications.

RESULTS

Increased *IFNAR2* expression is sufficient for the hypersensitivity to IFN-I observed in DS

We first confirmed previous findings of increased gene dosage of IFNAR1 and IFNAR2 in DS. As expected, we observed higher expression of *IFNAR1* and *IFNAR2* in human telomerase (hTERT)-immortalized fibroblasts derived from individuals with DS (DS), compared to those of healthy controls (HC), at both the mRNA and protein levels (Figures S1A and S1B). This elevated receptor expression resulted in increased proximal signaling in response to IFN-I stimulation, demonstrated by higher phosphorylation of signal transducers and activators of transcription (STATs), namely phospho-STAT1 and phospho-STAT2, in DS compared to HC fibroblasts (Figure 1A), as expected (Sullivan et al., 2016; Kong et al., 2020). Non-canonical signaling, as measured by the induction of STAT3 phosphorylation, was also increased in DS compared to wild-type controls (Figure 1A).

Downstream of the IFN-I signaling cascade, induction of IFN-stimulated genes (ISGs) *MX1*, *IFI27*, *IFIT1*, and *RSAD2* was correspondingly higher in DS fibroblasts compared to HC fibroblasts (Figures S1C and S1D). Of note, *MX1* is located on chromosome 21, therefore, its increased induction may not only be due to elevated IFN-I signaling but also to its increased copy number in DS fibroblasts. While elevation of IFNAR expression and STAT phosphorylation were subtle (<2-fold), ISG induction was more pronounced (up to 6-fold), suggestive of expected signal transduction amplification downstream of the receptor. This further supports the notion that, while the gene dosage of *IFNAR1* and *IFNAR2* is only 1.5× higher in trisomy 21 than in disomic controls, it can result in a profound hyperresponse to IFN-I in individuals with DS. Furthermore, the elevation in ISG expression was not only elevated compared to controls at peak induction but the presence of these ISGs was also sustained for up to a week after IFN-I stimulation, compared to only 3 days in controls (Figures S1E and S1F). Combined, these data confirm the IFNAR gene dosage effects in DS (Sullivan et al., 2016) and further suggest that these affect non-canonical signaling and persist over time.

As there are over 200 genes that are triplicated in DS and could play a role in the hyperresponse to IFN-I described above, we sought to delineate the impact of increased IFN-I receptor alone to this phenotype. We generated *IFNAR2* knockouts in HC fibroblasts and transduced them with a two-lentivirus system: a construct expressing *IFNAR2* under a tet-inducible promoter and a doxycycline-dependent reverse tetracycline-controlled trans-activator (rtTA) (Figures S2A–S2D). This resulted in a cell line in which *IFNAR2* amounts could be finely titrated with doxycycline treatment to match expression in HC and DS lines (Figure 1B). The intermediate dose of doxycycline (0.1 ug/mL) used corresponded to the HC surface expression, and the DS expression was between the intermediate (0.1 ug/mL) and high doses (0.5 ug/mL) of doxycycline (Figure 1B).

Increased dosage of IFNAR2 resulted in increased phospho-STAT1 in response to IFN-I (Figure 1C), leading to a strong correlation between *IFNAR2* expression and induction of phospho-STAT1 in the presence of IFN-I (Figure 1D). At the ISG level, higher *IFNAR2* expression was sufficient to replicate not only the short-term hyperinduction of *MX1*, *IFIT1*, and *USP18* seen in DS but it also resulted in the long-term persistence of these ISGs at the protein level, similar to what we determined in DS hTERTs (Figure 1E). While the induced IFNAR2 expression matched to HC and DS precisely corresponded to the respective levels of STAT1 phosphorylation, the ISGs induced were not perfectly matched, which suggests that some other factors may be at play downstream of the receptor. In conclusion, independent of trisomy 21, increased *IFNAR2* expression is sufficient to result in hyperresponse to IFN-I.

Initial hyperresponse to IFN-I underlies heightened IFN-I negative regulation

To prevent the potentially nefarious inflammatory effects of IFN-I, the pathway is tightly regulated by negative feedback mechanisms (Porritt and Hertzog, 2015). In the absence of this physiological process, significant pathology and even death occur (Meuwissen et al., 2016; Alsohime et al., 2020). This regulatory break of IFN-I signaling is carried out by several proteins, USP18 being one of the most potent of these negative regulators (François-Newton et al., 2011). USP18 is induced by IFN-I and binds to IFNAR2, thereby preventing Janus kinase 1 (JAK1) phosphorylation and downstream STAT phosphorylation. As a result, cells "primed" with an initial IFN-I stimulus become refractory to further IFN-I stimulation (François-Newton et al., 2011; Zhang et al., 2015).

Given that naïve DS fibroblasts hyperrespond to IFN-I stimulation, which results in increased production of the negative regulator USP18 (Figures S1C–S1F), we interrogated this negative feedback loop in DS. While naïve DS hTERT fibroblasts hyperrespond to IFN-I compared to control cells, when they were first "primed" with IFN-I, they in fact become hypo-responsive to a second IFN-I stimulus, as evidenced by decreased STAT1 and STAT2 phosphorylation compared to their HC counterparts (Figure 2A). IFNAR1 and IFNAR2 surface expression was not different between primed HC and DS fibroblasts (Figure S3A), therefore, this hypo-response is not mediated by differential receptor expression. The hypo-response is concomitant with

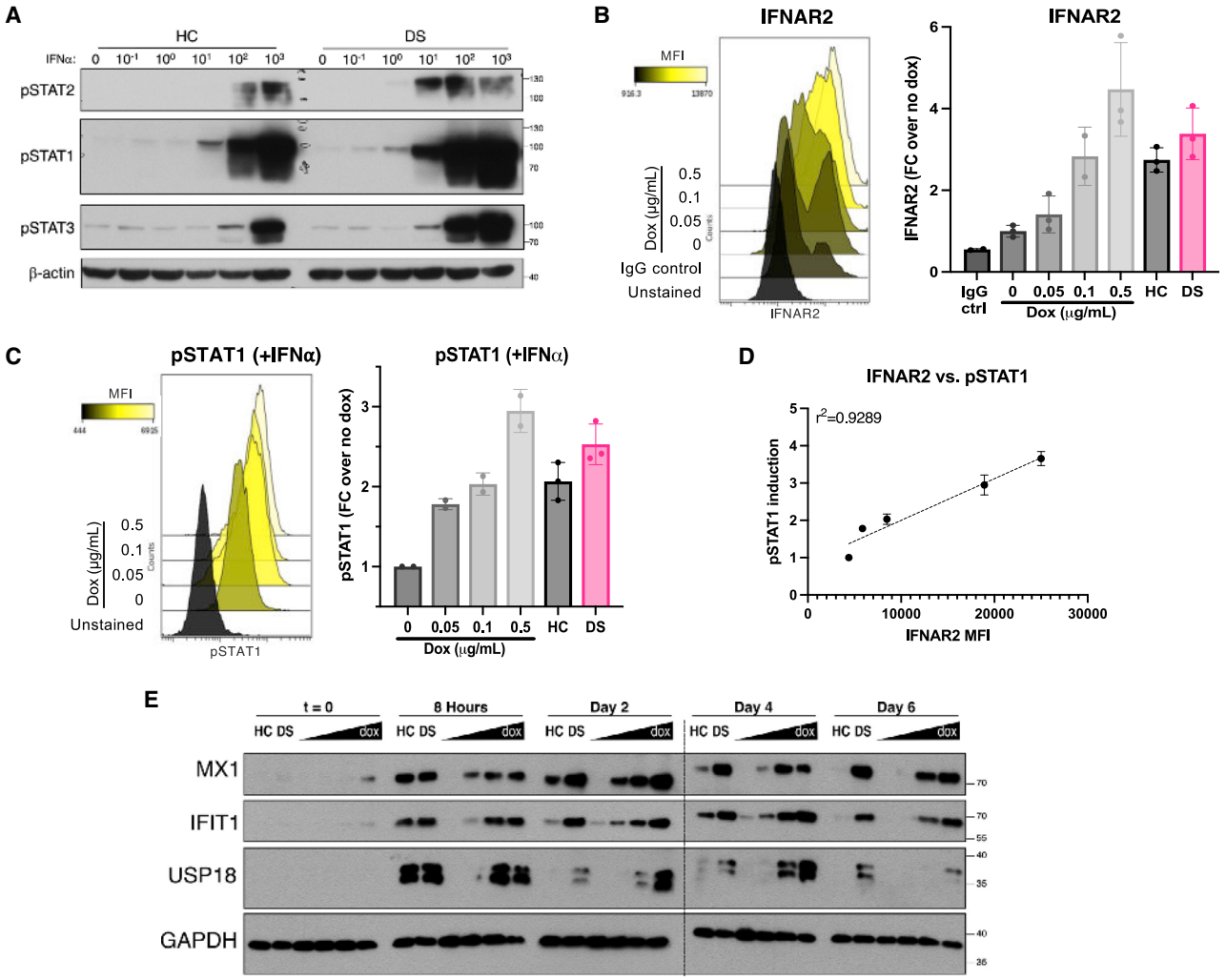

Figure 1. Hyperresponse to IFN-I in DS or with increased expression of *IFNAR2* alone

(A) Immunoblotting for STAT1, STAT2 and STAT3 phosphorylation in HC and DS hTERT-immortalized fibroblasts stimulated for 15 min with indicated doses of IFN-α (IU/mL). Result representative of fibroblasts derived from n = 3 HCs and n = 3 individuals with DS.

(B) Flow cytometry histogram and quantification of *IFNAR2* expression in hTERT *IFNAR2* knockouts complemented with doxycycline-inducible *IFNAR2*, treated with indicated amounts of doxycycline, and run in triplicates.

(C) Flow cytometry histogram and quantification of STAT1 phosphorylation in hTERTs complemented with doxycycline-inducible *IFNAR2*, treated with increasing amounts of doxycycline (0, 0.05, 0.1, and 0.5 mg/mL), and stimulated with IFN-α for 15 min (1000 IU/mL), run in duplicates.

(D) Correlation of IFNAR2 expression and STAT1 phosphorylation in hTERTs complemented with dox-inducible *IFNAR2* (r, Pearson correlation coefficient).

(E) Immunoblotting for ISG induction in hTERTs complemented with dox-inducible *IFNAR2,* treated with increasing amounts of doxycycline, followed by stimulation with IFN-α (10 IU/mL) for 8 h, wash, and rest for indicated times. Result representative of fibroblasts derived from n = 3 HCs and n = 3 individuals with DS.

* indicates samples were run on two separate gels. For all results in the figure, bars represent the mean ± SD. See also Figure S1 and S2.

elevated USP18 induction in primed DS cells compared to primed HC cells (Figure 2A). SOCS1, another known IFNAR negative regulator (Blumer et al., 2017), was not differentially induced in primed DS cells (Figure S3B), which suggests that it is not a key player in the increased negative regulation we observed in DS. Therefore, increased sensitivity to IFN-I can trigger excessive negative feedback, likely via increased USP18 induction, ultimately resulting in an immunosuppressive state.

Importantly, *IFNAR2* expression was sufficient to replicate this exacerbated refractory state. While *IFNAR2* expression positively correlated with STAT1 and STAT2 phosphorylation in naïve cells (Figures 1C and 2B, lanes 1–6), this relationship was inverted in primed cells: increasing *IFNAR2* resulted in a decrease of phospho-STATs (Figure 2B, lanes 7–12 and 2C, lanes 8–10). Like in DS fibroblasts, this heightened negative feedback is concomitant with the increase in USP18 expression in cells that express more IFNAR2 (Figures 2B and 2C). Furthermore, knocking out *USP18* reverts this phenotype so that primed cells remain responsive to a second IFN-I stimulation in an IFNAR2-dependent fashion (Figure 2D). Therefore, USP18 is necessary to induce IFNAR2-dose-dependent refractoriness to IFN-I.

We further explored the dynamics of IFN-induced negative feedback by adjusting the dose of IFN-I priming. The factors

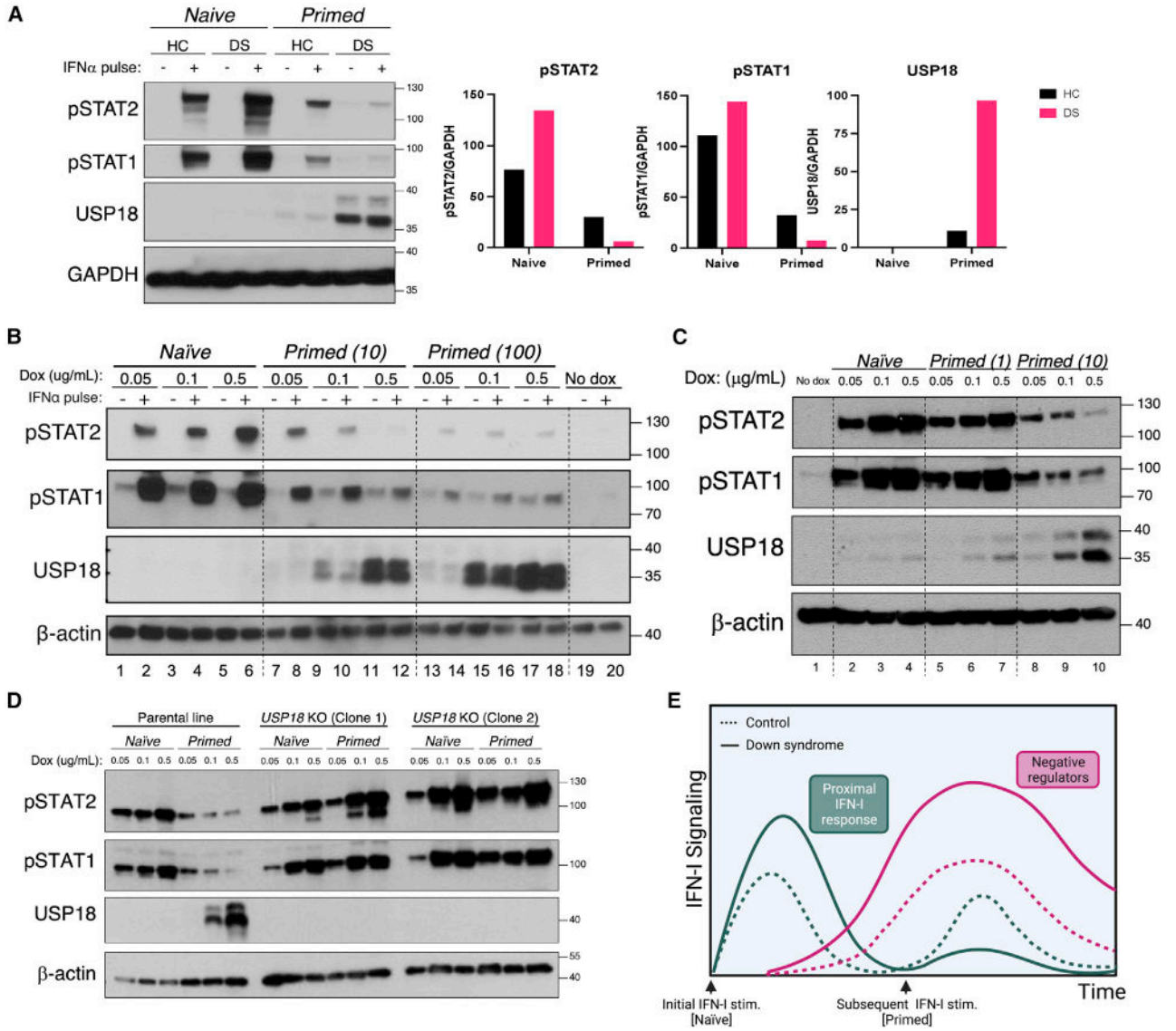

Figure 2. Initial hyperresponse to IFN-I underlies heightened IFN-I negative regulation

(A) Immunoblotting for STAT phosphorylation after stimulation for 15 min with IFN-α (100 IU/mL) of HC and DS hTERT-immortalized fibroblasts previously stimulated (Primed) or not (Naive) with a primary stimulus of IFN-α (10 IU/mL) for 12 h, washed, and allowed to rest for 36 h. Result representative of fibroblasts derived from n = 3 HCs and n = 3 individuals with DS.

(B) Immunoblotting for STAT phosphorylation after stimulation for 15 min with IFN-α (100 IU/mL) of *IFNAR2* knockouts complemented with doxycycline-inducible *IFNAR2*, treated with indicated amounts of doxycycline, and previously stimulated (Primed) or not (Naïve) with a primary stimulus of IFN-α (10 or 100 IU/mL). Results representative of n = 3 independent experiments.

(C) Immunoblotting for STAT phosphorylation after stimulation for 15 min with IFN-α (100 IU/mL) of *IFNAR2* knockouts complemented with doxycycline-inducible *IFNAR2*, treated with indicated amounts of doxycycline, and previously stimulated (Primed) or not (Naïve) with a primary stimulus of IFN-α (10 or 100 IU/mL).

(D) Immunoblotting for STAT phosphorylation after stimulation for 15 min with IFN-α (100 IU/mL) of *IFNAR2* knockouts complemented with doxycycline-inducible *IFNAR2*, treated with increasing concentrations of doxycycline and Primed (with 10 IU/mL IFN-α) or not (Naïve), in the presence (parental line) or absence (USP18 knockout Clones 1 and 2) of endogenous USP18.

(E) Diagram of hyper- and hypo-responses to IFN-I over time with subsequent stimulations in HC and DS individuals. See also Figure S3.

that dictate the response to a secondary IFN-I stimulus are not solely the quantity of receptors expressed but also the quantity of the ligands initially present. Priming with a low dose of IFN-I was not sufficient to induce significant negative regulation, regardless of IFNAR2 expression (Figure 2C, lanes 5–7). At this dose of priming (1 international unit [IU]/mL), the positive correlation between IFNAR2 expression and STAT phosphorylation remained even at re-stimulation, which was only reversed with priming at a higher dose of IFN-I (10 IU/mL) (Figure 2C, lanes 8–10). On the other end of the spectrum, the threshold of negative regulation was passed regardless of the amount of IFNAR2 if cells were primed with a high enough dose of IFN-I (100 IU/mL).

This resulted in a similar remarkable hypo-response to the secondary stimulus at all IFNAR2 expression levels (Figure 2B, lanes 13–18). In conclusion, the induction of IFN-I-negative feedback is a malleable process and depends on both the levels of receptor expressed and the dose of IFN-I priming (Figure S3). In our system, we showed that intermediate IFN-I priming opens a window of receptor-quantity-dependent temporal immune suppression. This phenotype could be reversed with a short-term pulse with Tofacitinib, a JAK inhibitor, which suggests that negative regulation is enacted by an IFN-induced protein and that transient immunosuppression can rescue cellular responsiveness to IFN-I (Figure S3C).

In all, our results confirm that higher expression of the IFN-I receptor can not only result in IFN-I mediated auto-inflammation in a naïve state but that it can also predispose cells to become refractory to IFN-I and thereby prolong the immunosuppressed state.

Myeloid cells from individuals with DS exhibit baseline IFN-I signaling and partial IFN-I desensitization

While cell lines are useful tools to test cytokine responses in a highly controlled manner, *ex vivo* studies in blood and peripheral blood mononuclear cells (PBMCs) are perhaps more physiologically reflective of the *in vivo* phenotype, at least at the time of sampling. We first evaluated whole blood from individuals with DS and age-matched controls by CyTOF (cytometry by time-of-flight) for two cell-surface-expressed ISGs, CD169/SIGLEC-1 and CD64/FcγRI. Both of these ISGs were elevated in the myeloid cells of individuals with DS in the absence of any exogenous stimulation (Figures 3A and 3B), suggesting the presence of basal IFN-I signaling. Additionally, and in accordance with other studies (Kong et al., 2020), phospho-STAT1 was detected by flow cytometry in the absence of stimulation in the $CD14^+$ monocytes of individuals with DS compared to their HC counterparts (Figure 3C), supporting the presence of IFN-I signaling at the steady-state in people with DS.

In line with this seemingly "lightly primed" state, there was no notable hyperresponse to IFN-I in DS myeloid cells, reflective of the plasticity of the system (Figure 3D). The IFN-I-stimulated induction of phospho-STAT1 over baseline was in fact lower in $CD14^+$ monocytes from people with DS compared to those of HCs (Figure 3E). Further downstream, the induction of ISGs *MX1*, *IFIT1*, and *IFI27* was also decreased in PBMCs derived from individuals with DS compared to HCs (Figure S3E). In accordance with these data, immunoblotting for USP18 revealed that this negative regulator was present at steady state in PBMCs derived from individuals with DS, but not those of HCs (Figure 3F), which indicates that these cells may be refractory to further IFN-I stimulation at baseline.

We postulate that basal phospho-STAT1, increased CD169 and CD64 surface expression, and an increased amount of USP18 are suggestive of prior exposure to IFN-I, so these cells are likely in a partial refractory state and thus not hyperresponding to subsequent IFN-I stimulation.

Increased IFN-I negative regulation underlies viral susceptibility

Individuals with DS are at higher risk of severe viral infections. This has been documented for RSV, IAV, and most recently for SARS-CoV-2 (Pérez-Padilla et al., 2010; Mitra et al., 2018; Malle et al., 2020; Clift et al., 2021). This risk is significant (adjusted hazard ratio of 10.39 for death from COVID-19) (Clift et al., 2021), but this viral susceptibility remains less stark than that of patients with complete deficiencies of *IFNAR1, IFNAR2, STAT1*, and *STAT2*, which often result in death from various viral insults (Boisson-Dupuis et al., 2012; Hambleton et al., 2013; Duncan et al., 2015; Taft and Bogunovic, 2018; Hernandez et al., 2019). In DS, while anatomical defects and dysregulated adaptive immune responses likely play a significant role in this susceptibility (Verstegen and Kusters, 2020; De Lausnay et al., 2021), we sought to determine if excessive IFN-I inflammation leading to more profound IFN-I-induced desensitization could be a contributing factor in this clinical phenotype.

To assess if refractoriness to IFN-I had an impact of viral susceptibility, we infected HC fibroblasts and HC fibroblasts constitutively over-expressing the IFN-I negative regulator USP18 (HC + USP18) with GFP-expressing IAV (IAV-GFP). While HC and HC + USP18 cells are infected at similar rates at baseline, stimulating the cells with IFN-I confers sizable protection to HCs, while HC + USP18 cells only have a modest, ~10% reduction in infection (Figure 4A). Thus, the IFN-I refractory state established by USP18 results in susceptibility to IAV infection.

We then tested whether the endogenous refractory state induced in HC cells, triggered as a part of a naturally occurring balance of protection from overt inflammation, can similarly have an impact on viral susceptibility. We infected naïve and primed HC hTERT fibroblasts with Zika virus (ZIKV) in absence or presence of an IFN-I stimulus. The IFN-I stimulus appreciably reduced infectivity in naïve cells (86% reduction in infection) (Figure 4B). Primed, unstimulated cells are still protected compared to naïve unstimulated cells, which shows that IFN-I confers some long-term resistance to cells, albeit waning as expected. Importantly, these primed cells do not better control the virus after a second IFN-I stimulus (Figure 4B). Despite the lingering protection from the IFN-I prime, these cells are more susceptible to the virus than naïve, stimulated cells. Thus, IFN-I priming prevents cells from mounting an antiviral state equivalent to that of naïve cells, making them more vulnerable to viral infection.

Next, we took advantage of our inducible system to study whether increased *IFNAR2* expression, which we have shown results in greater refractoriness to IFN-I, could result in more viral susceptibility. With low IFNAR2 expression, IFN-I treatment elicits a similar amount of viral protection in naïve and primed cells (28% and 22% decrease, respectively, compared to the unstimulated control) (Figure 4C, black boxes). By contrast, with high IFNAR2 expression, while IFN-I stimulation results in greater protection in their naïve state (47% reduction in infection), IFN-I has no additional effect in primed cells (no reduction in infection) (Figure 4C, pink boxes). This reflects the initial hyperresponse to IFN-I in naïve cells and subsequent hypo-response in primed cells that we described with increasing *IFNAR2* expression (Figure 2B). The heightened negative feedback in these cells thus results in an inability to harness IFN-I to potentiate an antiviral response.

As previously seen for ZIKV protection in HCs, in our *IFNAR2* system priming the cells with IFN-I results in long-lasting protection, decreasing the cellular infectivity compared to baseline (Figures 4D and 4E, solid black lines compared to dashed black

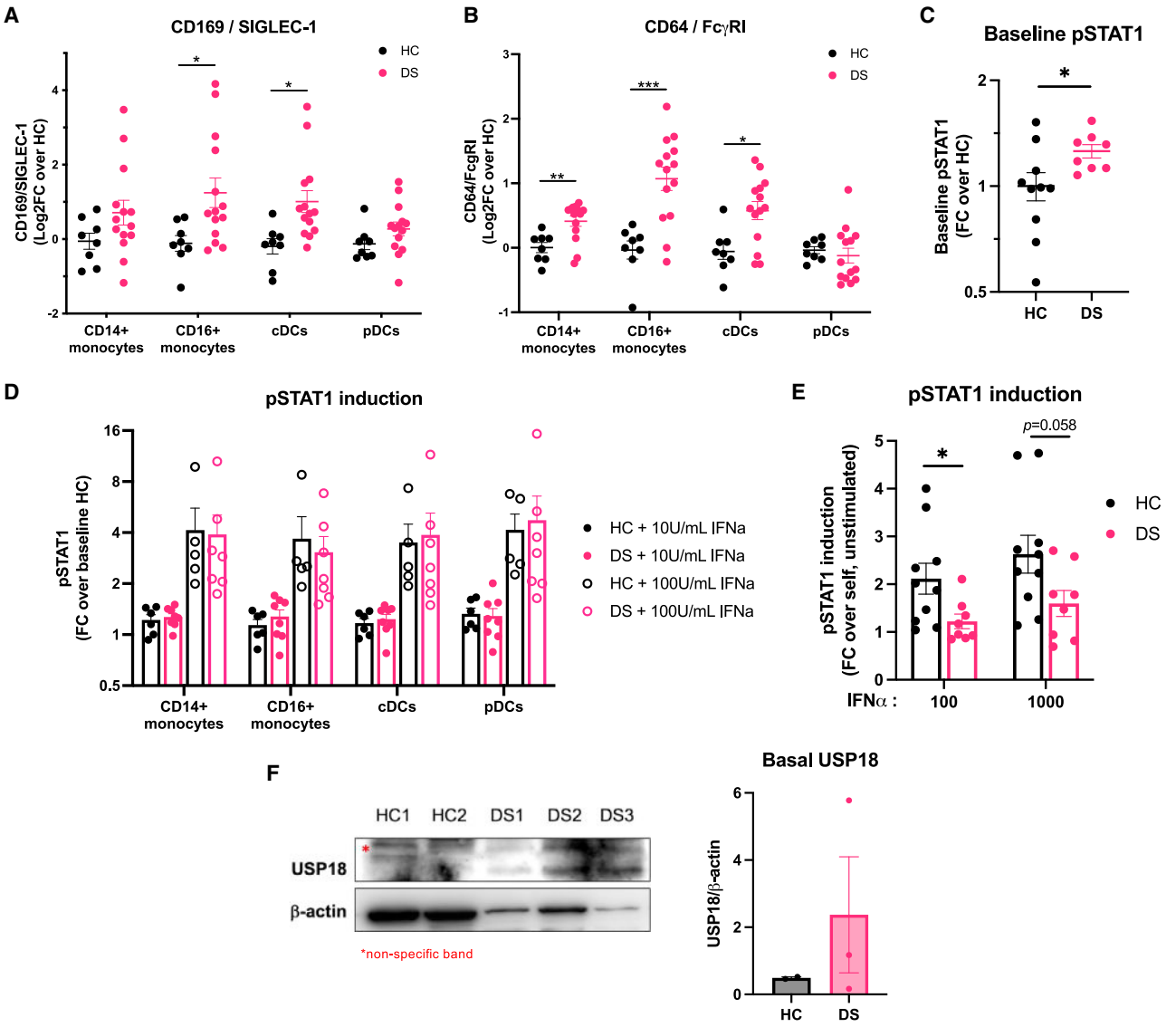

Figure 3. Basal IFN-I signaling and increased IFN-I negative regulation in monocytes from individuals with DS *ex vivo*

(A and B) CyTOF quantification of (A) CD169/SIGLEC-1 and (B) CD64/FcγRI at baseline in $CD14^+$ and $CD16^+$ monocytes and conventional (cDCs) and plasmacytoid dendritic cells (pDCs) from HC (n = 8) and DS (n = 14) whole blood.

(C) Flow cytometry quantification of baseline STAT1 phosphorylation in $CD14^+$ monocytes from HCs (n = 6) and individuals with DS (n = 7), expressed as fold-change over baseline healthy control.

(D) CyTOF quantification of STAT1 phosphorylation in $CD14^+$ and $CD16^+$ monocytes, cDCs, and pDCs from HC (n = 5) and DS (n = 7) whole blood stimulated for 15 min with 10 and 100 IU/mL IFN-α, expressed as fold-change over the average baseline of HCs.

(E) Flow cytometry quantification of STAT1 phosphorylation in $CD14^+$ monocytes after stimulation of HC (n = 6) and DS (n = 7) PBMCs for 15 min with indicated amounts of IFN-α (IU/mL), expressed as fold-change over each sample unstimulated.

(F) Immunoblotting and quantification for basal USP18 in total PBMCs from individuals with DS (n = 3) and age-matched controls (n = 2). * denotes a non-specific band. For all results in the figure, bars represent the mean ± SEM. Significance assessed by unpaired t tests, ns denotes $p > 0.05$, *$p \leq 0.05$; **$p \leq 0.005$; ***$p \leq 0.0005$. See also Figure S3.

lines). The ability to respond to a second stimulus, however, dictates whether this priming puts cells at higher risk of infection than naïve cells. Given their ability to remain responsive to subsequent IFN-I stimuli, low-IFNAR2 cells mount the greatest antiviral resistance with the combined effects of the prime and the restimulation (Figure 4D, pink dashed line). By contrast, with high amounts of IFNAR2 (DS-matched), primed cells that received an additional IFN-I stimulus (Figure 4E, pink dashed line) are more susceptible to IAV than naïve cells stimulated with IFN-I (Figure 4E, pink solid line and inlay, p = 0.04). Therefore, increasing *IFNAR2* expression results in heightened viral susceptibility in the context of repeated IFN-I stimuli or a continuous IFN-I inflammatory state, likely present in the clinical setting.

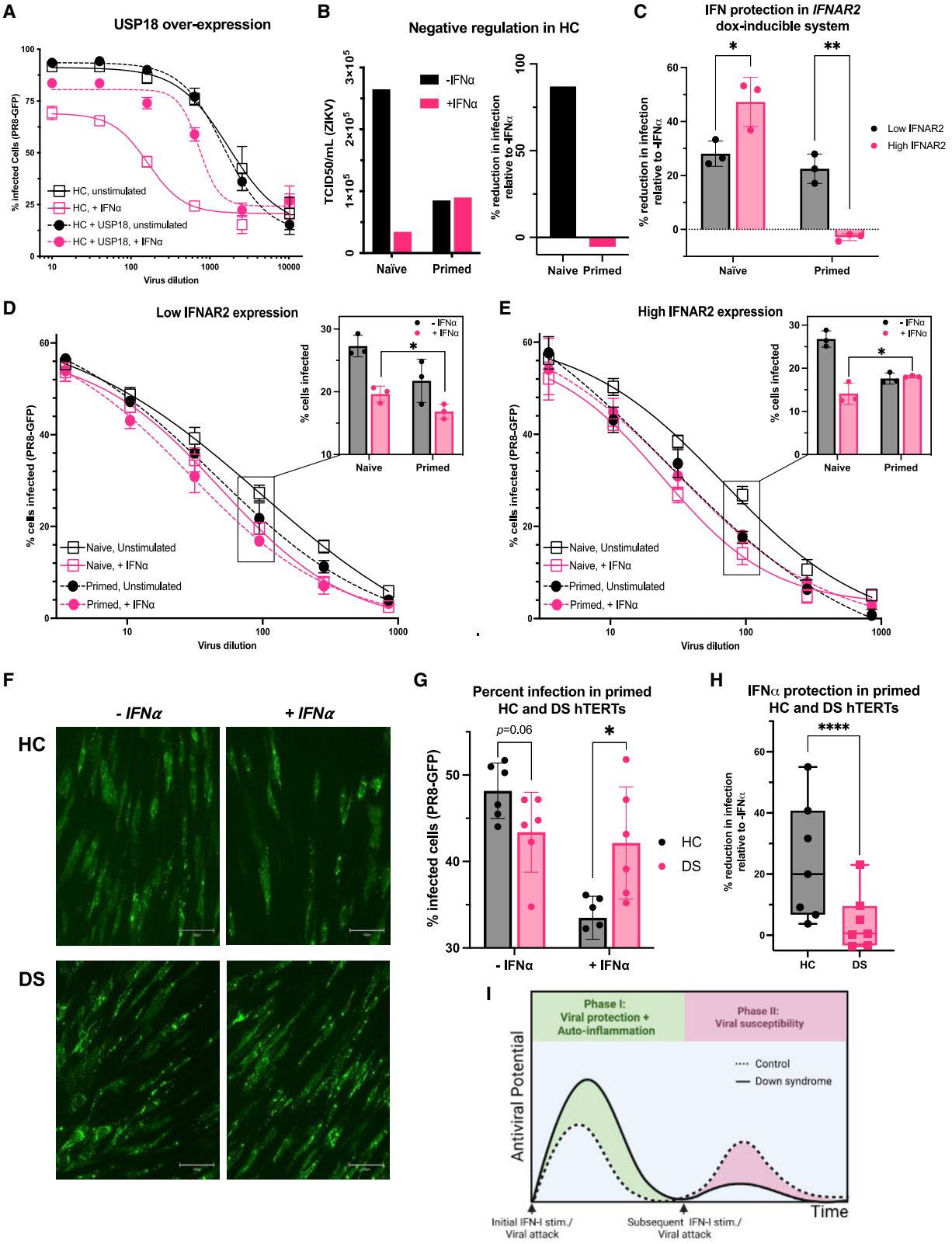

(legend on next page)

Finally, we turned to primed HC and DS hTERTs to test if the increased negative regulation observed in DS (Figure 2A) results in increased viral susceptibility. Although DS hTERTs are initially more sensitive to IFN-I, upon priming these cells exhibit resistance against IAV that is comparable to HC, although it did trend higher ($p = 0.06$) (Figures 4F and 4G). Perhaps more importantly, these DS primed cells cannot mount a second response to IFN-I, resulting in equal infectivity of IAV of about 43% of DS cells, whether primed or primed and additionally IFN-I stimulated (Figure 4G). In contrast, HC cell lines were protected via priming alone, which resulted in infectivity of IAV of about 48%, but when additional IFN-I was administered, IAV infectivity was further reduced to about 33% (Figure 4G). Additionally, at all IAV dilutions tested, IFN-I stimulation confers additional protection to primed HC hTERTs (24% reduction in infection on average compared to unstimulated cells) while DS hTERTs have a muted response to this second IFN-I stimulation (4% further reduction in infection) (Figure 4H). In conclusion, in the presence of additional IFN-I, primed HC cells are better protected from IAV infection than their DS counterparts ($p = 0.01$). Therefore, the IFN-I desensitization triggered in DS results in increased viral susceptibility compared to HCs.

DISCUSSION

Given the inborn nature of trisomy 21, its clinical immune presentation, and the mounting molecular evidence of genetic causation of immune pathology, DS belongs in the group of diseases collectively known as inborn errors of immunity (IEIs). Its main distinguishing feature from previously described IEIs is that it is not monogenic but rather monochromosomal. Furthermore, DS encompasses both autoinflammation and immune suppression.

The Mendelian IEIs provide valuable insight to frame our understanding of disturbances in the IFN-I pathway. IEIs causing chronic IFN-I signaling, termed Type I Interferonopathies (IFNopathies), cause a severe phenotype characterized by neurological disturbances and inflammatory features typically affecting the skin and/or the lungs (Rodero and Crow, 2016; Lee-Kirsch, 2017) and in some cases provide protection from viral infections. Previous studies have provided evidence that increased IFNAR gene dosage in DS results in inflammatory features that are comparable to a mild Type I IFNopathy, and recent epidemiologic data demonstrate that people with DS are protected from viral infections. However, DS also overlaps clinically with IEIs caused by defects in the IFN-I pathway, as individuals with DS are more susceptible to complications due to viral disease. Indeed, loss-of-function (LOF) mutations in *IFNAR1, IFNAR2, IRF7, IRF3*, and *STAT1* all result in severe viral susceptibility (Andersen et al., 2015; Duncan et al., 2015; Ciancanelli et al., 2015; Hernandez et al., 2019; Zhang et al., 2020). DS therefore corresponds to a mild form of both IFN-I gain-of-function (GOF) and LOF phenotypes.

Evidence stemming from these monogenic IEIs suggests that both excessive and insufficient IFN-I are pathogenic and that perturbations in duration and regulation of IFN-I signaling can also cause disease. The increase in IFNAR expression in DS puts individuals at risk of the negative effects of IFN-I at both ends of the spectrum. We show that the hyperactive IFN-I signaling cascade causes increased induction of the IFNAR negative regulator USP18, in turn hypersuppressing any subsequent response to IFN-I and effectively repressing further antiviral responses. Together with known defects in adaptive immunity in DS in both B and T cell compartments (Verstegen and Kusters, 2020) as well as anatomical anomalies of the respiratory tract such as laryngomalacia and tracheomalacia (De Lausnay et al., 2021), which all likely contribute to the susceptibility to infections in DS, the dampening of the innate antiviral response we describe here may explain why people with DS are more prone to severe viral infections. DS is therefore, in part, an inflammation-induced error of immunity.

While the mechanisms at play are still largely unknown, there is evidence in the general population that excessive and ill-timed IFN-I signaling can worsen infectious disease. Administration of recombinant IFN-I as a therapeutic in viral infections has repeatedly proven ineffective if administered at the inappropriate time or dose, including for HIV, hepatitis C virus (HCV), and SARS-CoV-2 among others (Asmuth et al., 2010; Teijaro, 2016; Kalil et al., 2021). In a cohort of patients with SARS, circulating IFN-I and ISG levels in fact correlated with disease severity (Cameron et al., 2007). Murine studies demonstrate that IFN-I is protective early in infection but later becomes pathogenic (Channappanavar et al., 2016, 2019; Park and Iwasaki, 2020), which was also recently reported in humans in the treatment of SARS-CoV-2, as IFN-β improved recovery time if administered

Figure 4. Increased IFN-I negative regulation underlies viral susceptibility

(A) HC hTERTs transduced or not with *USP18* were stimulated overnight with IFN-α (10 IU/mL) and infected with PR8-GFP for 8 h.

(B) ZIKV was titrated on HC HTERTs that were naïve or primed for 8 h with IFN-α (100 IU/mL), rested for 2.5 days, and restimulated with IFN-α (100 IU/mL) for 15 min, then infected with ZIKV 8 h later. To calculate the TCID50, infected wells were considered GFP+ if they displayed a mean intensity above the mean of the un-infected wells.

(C–E) hTERT *IFNAR2* knockouts complemented with doxycycline-inducible *IFNAR2* were treated with 0.05 ("Low IFNAR2") or 0.5 ("High IFNAR2") μg/mL doxycycline. Cells were initially treated (Primed) or not (Naïve) with a primary stimulus of IFN-α (10 IU/mL) for 8 h, allowed to rest for 4.5 days in DMEM+Dox, and restimulated with IFN-α (1000 IU/mL) for 15 min followed by 8 h rest and overnight infection with PR8-GFP. (C) Percent reduction in infection by IFN-I stimulation at 1:100 viral dilution. Raw percent infection at all viral dilutions tested (curves) and at 1:100 viral dilution (bar graphs) at (D) low and (E) high IFNAR2 levels.

(F–H) HC and DS hTERTs were initially treated with a primary stimulus of IFN-α (10 IU/mL) for 8 h, allowed to rest for 2.5 days, and restimulated with IFN-α (100 IU/mL) for 15 min followed by 8 h rest and overnight infection with PR8-GFP.

(F and G) (F) PR8-GFP fluorescence captured at 20× (scale bar denotes 100 μm) and (G) raw percent infection at 1:100 viral dilution.

(H) Percent reduction in infection by IFN-I stimulation at all viral dilutions tested. Results of $n = 2$ independent experiments.

(I) Diagram of auto-inflammatory and immuno-suppressed states over time with subsequent IFN-α stimulations in HC and DS individuals. For all results in the figure, bars represent the mean ± SD. Significance assessed by unpaired t tests, ns denotes $p > 0.05$, *$p \leq 0.05$; **$p \leq 0.005$; ***$p \leq 0.0005$.

early in the course of disease but proved ineffective or even deleterious when given at advanced stages of disease (Monk et al., 2021; WHO Solidarity Trial Consortium, 2021). These findings are in accordance with the notion that timing of IFN-I is key, as it can be protective against viral infection but IFN-I stimulation in "primed" cells is detrimental to viral control. For instance, administration of recombinant IFN-I before viral peak is protective in a murine model of Middle East Respiratory Syndrome, while late treatment results in nefarious inflammation and lethal pneumonia (Channappanavar et al., 2019). The role that IFN-I negative feedback plays in these observations remains to be investigated.

As both aspects of the typical physiologic IFN-I response are amplified in DS, an intermittent short-circuiting of IFNAR signaling via JAK inhibition or IFNAR blocking may help restore homeostasis. Put another way, transient immunosuppression may actually restore the ability of individuals with DS to fight off viral disease while ameliorating their hyperinflammation. Our experimental data support this notion, which warrants further investigation *ex vivo* and *in vivo*. So far, JAK inhibitor treatment is promising in curbing inflammatory symptoms in DS (Rachubinski et al., 2019; Pham et al., 2021), but it remains to be studied if this treatment improves the ability of individuals with DS to fend off viruses.

Limitations of the study

We acknowledge that important additional information surrounding IFN-I signaling in DS could be obtained from tissue biopsies at steady state, as well as by further *ex vivo* studies testing the response to IFN-I in virally infected individuals with DS. Furthermore, follow-up evaluations of the IFN-I response in the adaptive arm of the immune system and its impact on cell and antibody-mediated immunity are needed to fully explain epidemiological findings of infection-related morbidity and mortality in DS.

STAR★METHODS

Detailed methods are provided in the online version of this paper and include the following:

- KEY RESOURCES TABLE
- RESOURCE AVAILABILITY
  - Lead contact
  - Materials availability
  - Data and code availability
- EXPERIMENTAL MODEL AND SUBJECT DETAILS
  - Human samples
  - Cell lines
- METHOD DETAILS
  - Cloning
  - CRISPR editing
  - RNA isolation and quantitative PCR
  - IFNAR negative regulation
  - Protein assays
  - Flow cytometry
  - Mass cytometry
  - Viral challenges

SUPPLEMENTAL INFORMATION

Supplemental information can be found online at https://doi.org/10.1016/j.immuni.2022.09.007.

ACKNOWLEDGMENTS

We thank all individuals and their families for their participation. We thank Adeeb Rahman, Daniel Geanon, and Geoffrey Kelly from the Human Immune Monitoring Center at the Icahn School of Medicine for their technical assistance. We also thank Sandra Pellegrini for sharing reagents. This study was funded by the National Institute of Allergy and Infectious Diseases grants R01AI150300, R01AI151029, R01AI148963, and R01AI150300-01S1. L.M. was supported by T32 training grant T32HD075735.

AUTHOR CONTRIBUTIONS

L.M. designed and performed most of the experiments, analyzed the data, and wrote the manuscript. M.M.F. performed multiple experiments and analyzed data. S.B. and A.R. generated and maintained cell lines and helped perform experiments. D. Bush recruited patients and edited the manuscript. D. Bogunovic supervised the work, wrote the manuscript, and helped design the experiments and analyze the data.

DECLARATION OF INTERESTS

D. Bogunovic is the founder of Lab11 Therapeutics.

INCLUSION AND DIVERSITY

We worked to ensure gender balance in the recruitment of human subjects. We worked to ensure ethnic or other types of diversity in the recruitment of human subjects. We worked to ensure that the study questionnaires were prepared in an inclusive way. While citing references scientifically relevant for this work, we also actively worked to promote gender balance in our reference list. The author list of this paper includes contributors from the location where the research was conducted who participated in the data collection, design, analysis, and/or interpretation of the work.

Received: March 13, 2022
Revised: July 4, 2022
Accepted: September 12, 2022
Published: October 14, 2022

REFERENCES

Alsohime, F., Martin-Fernandez, M., Temsah, M.H., Alabdulhafid, M., Le Voyer, T., Alghamdi, M., Qiu, X., Alotaibi, N., Alkahtani, A., Buta, S., et al. (2020). JAK Inhibitor Therapy in a Child with Inherited USP18 Deficiency. N. Engl. J. Med. *382*, 256–265. https://doi.org/10.1056/NEJMoa1905633.

Andersen, L.L., et al. (2015). Functional IRF3 deficiency in a patient with herpes simplex encephalitis. J. Exp. Med. *212*, 1371. The Rockefeller University Press. https://doi.org/10.1084/JEM.20142274.

Asmuth, D.M., et al. (2010). Safely, tolerability, and mechanisms of antiretroviral activity of pegylated interferon alfa-2a in HIV-1monoinfected participants: A phase II clinical trial. JID (J. Infect. Dis.) *201*, 1686–1696. Oxford University Press. https://doi.org/10.1086/652420.

Bcheraoui, C. el, Mokdad, A.H., Dwyer-Lindgren, L., Bertozzi-Villa, A., Stubbs, R.W., Morozoff, C., Shirude, S., Naghavi, M., and Murray, C.J.L. (2018). Trends and Patterns of Differences in Infectious Disease Mortality Among US Counties, 1980-2014. *JAMA*. American Medical Association *319*, 1248–1260. https://doi.org/10.1001/JAMA.2018.2089.

Blumer, T., Coto-Llerena, M., Duong, F.H.T., and Heim, M.H. (2017). SOCS1 is an inducible negative regulator of interferon λ (IFN-λ)–induced gene expression *in vivo*. J. Biol. Chem. *292*, 17928–17938. https://doi.org/10.1074/JBC.M117.788877.

Boisson-Dupuis, S., et al. (2012). Inborn errors of human STAT1: allelic heterogeneity governs the diversity of immunological and infectious phenotypes.

Curr. Opin. Immunol. *24*, 364. Elsevier. https://doi.org/10.1016/J.COI.2012.04.011.

Bruijn, M., et al. (2007). High incidence of acute lung injury in children with Down syndrome. Intensive Care Med. *33*, 2179–2182. Springer. https://doi.org/10.1007/s00134-007-0803-z.

Bull, M. J. (2020) 'Down syndrome', N. Engl. J. Med. Edited by A. H. Ropper. Massachusetts Medical Society, 382, pp. 2344–2352. https://doi.org/10.1056/NEJMra1706537.

Cameron, M.J., Ran, L., Xu, L., Danesh, A., Bermejo-Martin, J.F., Cameron, C.M., Muller, M.P., Gold, W.L., Richardson, S.E., Poutanen, S.M., et al. (2007). Interferon-mediated immunopathological events are associated with atypical innate and adaptive immune responses in patients with severe acute respiratory syndrome', *Journal of virology*. J. Virol. *81*, 8692–8706. https://doi.org/10.1128/JVI.00527-07.

Channappanavar, R., et al. (2016). Dysregulated Type I Interferon and Inflammatory Monocyte-Macrophage Responses Cause Lethal Pneumonia in SARS-CoV-Infected Mice. Cell Host Microbe *19*, 181–193. Cell Press. https://doi.org/10.1016/j.chom.2016.01.007.

Channappanavar, R., Fehr, A.R., Zheng, J., Wohlford-Lenane, C., Abrahante, J.E., Mack, M., Sompallae, R., McCray, P.B., Jr., Meyerholz, D.K., and Perlman, S. (2019). IFN-I response timing relative to virus replication determines MERS coronavirus infection outcomes'. J. Clin. Invest. *129*, 3625–3639. https://doi.org/10.1172/JCI126363.

Ciancanelli, M.J., Huang, S.X.L., Shishido, H., Yang, Z., Rooney, L.A., Barral, J.M., Skach, W.R., Trouillet, C., Schmolke, M., Albrecht, R.A., et al. (2015). Life-threatening influenza and impaired interferon amplification in human IRF7 deficiency. Science *348*, 444–448. https://doi.org/10.1126/science.aaa3974.

Clift, A.K., et al. (2021). COVID-19 Mortality Risk in Down Syndrome: Results From a Cohort Study of 8 Million Adults. Ann. Intern. Med. M20–M4986. American College of Physicians. https://doi.org/10.7326/M20-4986.

De Lausnay, M., et al. (2021). Pulmonary Complications in Children with Down Syndrome: A Scoping Review. Paediatr. Respir. Rev. https://doi.org/10.1016/j.prrv.2021.04.006.

Duncan, C.J.A., Mohamad, S.M.B., Young, D.F., Skelton, A.J., Leahy, T.R., Munday, D.C., Butler, K.M., Morfopoulou, S., Brown, J.R., Hubank, M., et al. (2015). Human IFNAR2 deficiency: Lessons for antiviral immunity', *Science translational medicine*. Sci. Transl. Med. *7*, 307ra154. https://doi.org/10.1126/scitranslmed.aac4227.

Fitzpatrick, V., Rivelli, A., Chaudhari, S., Chicoine, L., Jia, G., Rzhetsky, A., and Chicoine, B. (2022). Prevalence of Infectious Diseases Among 6078 Individuals With Prevalence of Infectious Diseases Among 6078 Individuals With Down Syndrome in the United States. J. Patient. Cent. Res. Rev. *9*, 64–69. https://doi.org/10.17294/2330-0698.1876.

François-Newton, V., et al. (2011). In 'USP18-Based Negative Feedback Control Is Induced by Type I and Type III Interferons and Specifically Inactivates Interferon α Response', *PLoS ONE*, *6*, K.L. Mossman, ed. (Public Library of Science). https://doi.org/10.1371/journal.pone.0022200.

Geanon, D., Lee, B., Kelly, G., Handler, D., Upadhyaya, B., Leech, J., Herbinet, M., Del Valle, D., Gnjatic, S., Kim-Schulze, S., et al. (2020). A Streamlined CyTOF Workflow To Facilitate Standardized Multi-Site Immune Profiling of COVID-19 Patients. Preprint at medRxiv. 2020.06.26.20141341. https://doi.org/10.1101/2020.06.26.20141341.

Hambleton, S., Goodbourn, S., Young, D.F., Dickinson, P., Mohamad, S.M.B., Valappil, M., McGovern, N., Cant, A.J., Hackett, S.J., Ghazal, P., et al. (2013). STAT2 deficiency and susceptibility to viral illness in humans. Proc. Natl. Acad. Sci. USA. *110*, 3053–3058. https://doi.org/10.1073/pnas.1220098110.

Hernandez, N., Bucciol, G., Moens, L., Le Pen, J., Shahrooei, M., Goudouris, E., Shirkani, A., Changi-Ashtiani, M., Rokni-Zadeh, H., Sayar, E.H., et al. (2019). Inherited IFNAR1 deficiency in otherwise healthy patients with adverse reaction to measles and yellow fever live vaccines. J. Exp. Med. *216*, 2057–2070. https://doi.org/10.1084/jem.20182295.

Kalil, A.C., et al. (2021). Efficacy of interferon beta-1a plus remdesivir compared with remdesivir alone in hospitalised adults with COVID-19: a double-bind, randomised, placebo-controlled, phase 3 trial. Lancet Respir. Med. *9*, 1365–1376. Elsevier Ltd. https://doi.org/10.1016/S2213-2600(21)00384-2.

Kong, X.-F., Worley, L., Rinchai, D., Bondet, V., Jithesh, P.V., Goulet, M., Nonnotte, E., Rebillat, A.S., Conte, M., Mircher, C., et al. (2020). Three Copies of Four Interferon Receptor Genes Underlie a Mild Type I Interferonopathy in Down Syndrome. J. Clin. Immunol. *40*, 807–819. https://doi.org/10.1007/s10875-020-00803-9.

Lee-Kirsch, M.A. (2017). The Type I Interferonopathies. Annu. Rev. Med. 297–315. https://doi.org/10.1146/annurev-med-050715-104506.

Mai, C.T., et al. (2019). National population-based estimates for major birth defects, 2010–2014. Birth Defects Research, *111* (John Wiley and Sons Inc.), pp. 1420–1435. https://doi.org/10.1002/bdr2.1589.

Malle, L., Gao, C., Hur, C., Truong, H.Q., Bouvier, N.M., Percha, B., Kong, X.F., and Bogunovic, D. (2020). Individuals with Down syndrome hospitalized with COVID-19 have more severe disease. Genet. Med. *23*, 576–580. https://doi.org/10.1038/s41436-020.

Malle, L., Bastard, P., Martin-Nalda, A., Carpenter, T., Bush, D., Patel, R., Colobran, R., Soler-Palacin, P., Casanova, J.L., Gans, M., et al. (2021). Atypical Inflammatory Syndrome Triggered by SARS-CoV-2 in Infants with Down Syndrome. J. Clin. Immunol. *41*, 1457–1462. https://doi.org/10.1007/S10875-021-01078-4.

McQuin, C., Goodman, A., Chernyshev, V., Kamentsky, L., Cimini, B.A., Karhohs, K.W., Doan, M., Ding, L., Rafelski, S.M., Thirstrup, D., et al. (2018). CellProfiler 3.0: Next-generation image processing for biology. PLoS Biol. *16*, e2005970. https://doi.org/10.1371/journal.pbio.2005970.

Meuwissen, M.E.C., et al. (2016). Human USP18 deficiency underlies type 1 interferonopathy leading to severe pseudo-TORCH syndrome. J. Exp. Med. *213*, 1163–1174. Rockefeller University Press. https://doi.org/10.1084/jem.20151529.

Mitra, S., El Azrak, M., McCord, H., and Paes, B.A. (2018). Hospitalization for Respiratory Syncytial Virus in Children with Down Syndrome Less than 2 Years of Age: A Systematic Review and Meta-Analysis. J. Pediatr. *203*, 92–100.e3. https://doi.org/10.1016/J.JPEDS.2018.08.006.

Monk, P.D., Marsden, R.J., Tear, V.J., Brookes, J., Batten, T.N., Mankowski, M., Gabbay, F.J., Davies, D.E., Holgate, S.T., Ho, L.P., et al. (2021). Safety and efficacy of inhaled nebulised interferon beta-1a (SNG001) for treatment of SARS-CoV-2 infection: a randomised, double-blind, placebo-controlled, phase 2 trial. Lancet Respir. Med. *9*, 196–206. https://doi.org/10.1016/S2213-2600(20)30511-7.

O'Leary, L., Hughes-McCormack, L., Dunn, K., and Cooper, S.A. (2018). Early death and causes of death of people with Down syndrome: A systematic review. J. Appl. Res. Intellect. Disabil. *31*, 687–708. https://doi.org/10.1111/jar.12446.

Park, A., and Iwasaki, A. (2020). Type I and Type III Interferons - Induction, Signaling, Evasion, and Application to Combat COVID-19. Cell Host Microbe *27*, 870–878. https://doi.org/10.1016/j.chom.2020.05.008.

Pérez-Padilla, R., Fernández, R., García-Sancho, C., Franco-Marina, F., Aburto, O., López-Gatell, H., and Bojórquez, I. (2010). Pandemic (H1N1) 2009 Virus and Down syndrome patients. Emerg. Infect. Dis. *16*, 1312–1314. https://doi.org/10.3201/eid1608.091931.

Pham, A.T., Rachubinski, A.L., Enriquez-Estrada, B., Worek, K., Griffith, M., and Espinosa, J.M. (2021). JAK inhibition for treatment of psoriatic arthritis in Down syndrome. Rheumatology *60*, e309–e311. https://doi.org/10.1093/rheumatology/keab203.

Porritt, R.A., and Hertzog, P.J. (2015). Dynamic control of type I IFN signalling by an integrated network of negative regulators. Trends Immunol. *36*, 150–160. https://doi.org/10.1016/j.it.2015.02.002.

Rachubinski, A.L., Estrada, B.E., Norris, D., Dunnick, C.A., Boldrick, J.C., and Espinosa, J.M. (2019). CASE REPORT Janus kinase inhibition in Down syndrome: 2 cases of therapeutic benefit for alopecia areata. JAAD Case Rep. *5*, 365–367. https://doi.org/10.1016/j.jdcr.2019.02.007.

Rodero, M.P., and Crow, Y.J. (2016). Type I interferon-mediated monogenic autoinflammation: The type I interferonopathies, a conceptual overview. J. Exp. Med. *213*, 2527–2538. https://doi.org/10.1084/jem.20161596.

Santoro, S.L., Chicoine, B., Jasien, J.M., Kim, J.L., Stephens, M., Bulova, P., and Capone, G. (2021). Pneumonia and respiratory infections in Down syndrome: A scoping review of the literature. Am. J. Med. Genet. *185*, 286–299. Part A. https://doi.org/10.1002/AJMG.A.61924.

Sullivan, K.D., Lewis, H.C., Hill, A.A., Pandey, A., Jackson, L.P., Cabral, J.M., Smith, K.P., Liggett, L.A., Gomez, E.B., Galbraith, M.D., et al. (2016). Trisomy 21 consistently activates the interferon response. Elife *5*, e16220. https://doi.org/10.7554/eLife.16220.001.

Taft, J., and Bogunovic, D. (2018). The Goldilocks Zone of Type I IFNs: Lessons from Human Genetics. J. Immunol. *201*, 3479–3485. https://doi.org/10.4049/jimmunol.1800764.

Teijaro, J.R. (2016). Type I interferons in viral control and immune regulation. Current Opinion in Virology, *16* (Elsevier), p. 31. https://doi.org/10.1016/J.COVIRO.2016.01.001.

Uppal, H., Chandran, S., and Potluri, R. (2015). Risk factors for mortality in Down syndrome. J. Intellect. Disabil. Res. *59*, 873–881. Blackwell Publishing Ltd. https://doi.org/10.1111/jir.12196.

Verstegen, R.H.J., and Kusters, M.A.A. (2020). Inborn Errors of Adaptive Immunity in Down Syndrome. J. Clin. Immunol. 791–806. Springer. https://doi.org/10.1007/s10875-020-00805-7.

WHO Solidarity Trial Consortium (2021). Repurposed Antiviral Drugs for Covid-19 — Interim WHO Solidarity Trial Results. N. Engl. J. Med. Overseas. Ed. *384*, 497–511. New England Journal of Medicine. https://doi.org/10.1056/nejmoa2023184.

Zhang, Q., Bastard, P., Liu, Z., Le Pen, J., Moncada-Velez, M., Chen, J., Ogishi, M., Sabli, I.K.D., Hodeib, S., Korol, C., et al. (2020). Inborn errors of type I IFN immunity in patients with life-threatening COVID-19. Science *370*, eabd4570. https://doi.org/10.1126/science.abd4570.

Zhang, X., Bogunovic, D., Payelle-Brogard, B., Francois-Newton, V., Speer, S.D., Yuan, C., Volpi, S., Li, Z., Sanal, O., Mansouri, D., et al. (2015). Human intracellular ISG15 prevents interferon-α/β over-amplification and auto-inflammation. Nature *517*, 89–93. https://doi.org/10.1038/nature13801.

STAR★METHODS

KEY RESOURCES TABLE

REAGENT or RESOURCE	SOURCE	IDENTIFIER
Antibodies		
Mouse anti-STAT1 Clone C-111	Santa Cruz Biotechnology	Cat No. sc417
Rabbit anti-STAT2	Millipore Sigma	Cat No. 06502
Rabbit anti-phospho-Tyr 701-STAT1 Clone 58D6	Cell Signaling Technology	Cat No. 9167
Rabbit anti-phospho-Tyr-689-STAT2 Clone D3P2P	Cell Signaling Technology	Cat No. 88410
Rabbit anti-USP18 Clone D4E7	Cell Signaling Technology	Cat No. 4813
Rabbit anti-β-actin Clone AC026	ABclonal	Cat No. AC026
Mouse anti-GAPDH Clone 6C5	Millipore	Cat No. MAB374
Rabbit anti-IFIT1 Clone D2X9Z	Cell Signaling Technology	Cat No. 14769
Rabbit polyclonal anti-MX1	Abcam	Cat No. ab95926
Rabbit polyclonal anti-SOCS1	Thermo Fisher Scientific	Cat No. PA5-27239
Goat anti-mouse IgG HRP-conjugated	Southern Biotech	Cat No. 101005
Goat anti-rabbit IgG HRP-conjugated	Southern Biotech	Cat No. 403005
anti-CD16 AF647-conjugated Clone 3G8	Biolegend	Cat No. 302023
anti-CD56 BV711-conjugated Clone 5.1H11	Biolegend	Cat No. 362541
anti-CD19 AF700-conjugated Clone HIB19	Biolegend	Cat No. 302225
anti-CD14 AF488-conjugated Clone M5E2	Biolegend	Cat No. 301811
anti-CD3 BV510-conjugated Clone OKT3	Biolegend	Cat No. 317331
anti-Stat1 (pY701) PE-conjugated, Clone 4A	BD	Cat No. 612564
anti-IFNAR1, Clone MARI-5A3	Millipore Sigma	Cat. No. 04-151
Anti-IFNAR1, Clone AA3	Laboratory of Sandra Pellegrini	N/A
anti-IFNAR2, Clone MMHAR-2	PBL	Cat No. 21385-1
rat anti-mouse IgG (H + L), biotin conjugated	Thermo Fisher	Cat No. 13-4013-85
Streptavidin, PE-conjugated	Thermo Fisher	Cat No. S866
anti-CD45 89Y-conjugated Clone HI30	Fluidigm	Cat No.3089003B
anti-CD57 113In-conjugated Clone HCD57	Biolegend	Cat No.322302
anti-CD11c 115In-conjugated Clone Bu15	Biolegend	Cat No.337202
anti-IgD 141Pr-conjugated Clone IA6-02	Biolegend	Cat No.348202
anti-CD19 142Nd-conjugated Clone HIB19	Biolegend	Cat No.302202
anti-CD45RA 143Nd-conjugated Clone HI100	Biolegend	Cat No.304102
anti-CD141 144Nd-conjugated Clone M80	Biolegend	Cat No.344102
anti-CD4 145Nd-conjugated Clone RPA-T4	Biolegend	Cat No.300502
anti-CD8 146Nd-conjugated Clone RPA-T8	Biolegend	Cat No.301002
anti-CD20 147Sm-conjugated Clone 2H7	Biolegend	Cat No.302302
anti-CD16 148Nd-conjugated Clone 3G8	Biolegend	Cat No.302014
anti-CD127 149Sm-conjugated Clone A019D5	Fluidigm	Cat No.3149011B
anti-CD1c 150Nd-conjugated Clone L161	Biolegend	Cat No.331502
anti-CD123 151Eu-conjugated Clone 6H6	Biolegend	Cat No.306002
anti-CD66b 152Sm-conjugated Clone G10F5	Biolegend	Cat No.305102
anti-CD86 154Sm-conjugated Clone IT2.2	Biolegend	Cat No.305410
anti-CD27 155Gd-conjugated Clone O323	Biolegend	Cat No.302802
anti-CD33 158Gd-conjugated Clone WM53	Biolegend	Cat No.303402
anti-CD24 159Tb-conjugated Clone ML5	Biolegend	Cat No.311102
anti-CD14 160Gd-conjugated Clone M5E2	Biolegend	Cat No.301810
anti-CD56 161Dy-conjugated Clone B159	BD Biosciences	Cat No.555513

(*Continued on next page*)

Continued

REAGENT or RESOURCE	SOURCE	IDENTIFIER
anti-CD169 162Dy-conjugated Clone 7-239	Biolegend	Cat No.346002
anti-CD69 164Dy-conjugated Clone FN50	Biolegend	Cat No.310902
anti-CD64 165Ho-conjugated Clone 10.1	Biolegend	Cat No.305047
anti-CD3 168Er-conjugated Clone UCHT1	Biolegend	Cat No.300402
anti-CD38 170Er-conjugated Clone HB-7	Biolegend	Cat No.356602
anti-CD161 171Yb-conjugated Clone HP-3G10	Biolegend	Cat No.339902
anti-HLADR 174Yb-conjugated Clone L243	Biolegend	Cat No.307602
anti-pSTAT5 147 Sm-conjugated Clone 47	Fluidigm	Cat No.3147012A
anti-pSTAT6 149 Sm-conjugated Clone 18/P-Stat6	Fluidigm	Cat No.3149004A
anti-pSTAT1 153 Eu-conjugated Clone 4a	Fluidigm	Cat No.3153005A
anti-pp38 156 Gd-conjugated Clone D3F9	Fluidigm	Cat No.3156002A
anti-pSTAT3 158 Gd-conjugated Clone 4/P-Stat3	Fluidigm	Cat No.3158005A
anti-pMAPKAP2 159 Tb-conjugated Clone 27B7	Fluidigm	Cat No.3159010A
anti-STAT3 165 Ho-conjugated Clone 124H6	Fluidigm	Cat No.3173003A
anti-STAT1 169 Tm-conjugated Clone 10C4B40	Biolegend	Cat No.661002
anti-pERK 171 Yb-conjugated Clone D13.14.4E	Fluidigm	Cat No.3171010A
anti-pS6 175 Lu-conjugated Clone N7-548	Fluidigm	Cat No.3175009A
anti-Flavivirus Group Antigen, Clone D1-4G2-4-15	Millipore	MAB10216
Goat anti Mouse IgG (H + L) Secondary Antibody, Alexa Fluor 647	Thermo Fisher	Cat No. A21235
Bacterial and virus strains		
DH5-Alpha Competent E. Coli	Molecular Cloning Laboratories	Cat No. DA-196
PR8-GFP, Influenza A/PR/8/34 (PR8) virus (H1N1)	Laboratory of Adolfo Garcia-Sastre	N/A
ZIKV, strain PRVABC59, GenBank: KU501215.1	Laboratory of Matthew Evans	N/A
Biological samples		
Human whole blood samples	Various institutions	N/A
HC-derived primary dermal fibroblasts	ATCC	Cat No. CRL2088
HC-derived primary dermal fibroblasts	Coriell institute	Cat No. GM03440, GM08447
DS-derived primary dermal fibroblasts	ATCC	Cat No. CCL54
DS-derived primary dermal fibroblasts	Coriell institute	Cat No. AG08942, GM04616
Chemicals, peptides, and recombinant proteins		
Intron-A Recombinant Interferon Alpha-2b	Merck Pharmaceuticals	Cat No. NDC0085057102
Proteomic Stabilizer Prot1	SMART TUBE Inc	Cat No. 501351691
Heparin	Sigma	Cat No. 201060
Osmium tetroxide (99.9%)	ACROS organics	Cat No. 191180010
Discovery Ultra antibody block	Roche	Cat No. 760-4204
Pierce ECL Western Blotting Substrate	Thermo Fisher Scientific	Cat No. 32106
Pierce Super-Signal West Pico PLUS Chemiluminescent Substrate	Thermo Fisher Scientific	Cat No. 34580
RIPA Lysis and Extraction Buffer	Thermo Fisher Scientific	Cat No. 89901
Protease/Phosphatase Inhibitor Cocktail	Cell Signaling Technologies	Cat No. 5872
Macherey-Nagel RNA Isolation, RA1 Lysis Buffer	Thermo Fisher Scientific	Cat No. 10335832
Cytofix/Cytoperm Fixation/Permeabilization Solution	BD	Cat No. 554714
Doxycycline hyclate	Sigma-Aldrich	Cat No. D9891
Alt-R S.p. Cas9 Nuclease V3	IDT	Cat No. 1081058
Histopaque 1077	Millipore Sigma	Cat No. 10771-500
Critical commercial assays		
Direct-zol RNA Microprep	Zymo Research	Cat No. R2060
RNeasy RNA Isolation Kit	Qiagen	Cat No. 74106

(*Continued on next page*)

Continued

REAGENT or RESOURCE	SOURCE	IDENTIFIER
Applied Biosystems High-Capacity cDNA Reverse Transcription Kit	Thermo Fisher Scientific	Cat No. 4368814
TaqMan Universal Master Mix II with UNG	Thermo Fisher Scientific	Cat No. 4440039
Infusion HD	Takara Bio	Cat No. 638909
CloneAmp HiFi PCR Premix	Takara Bio	Cat No. 639298
MycoAlert PLUS Mycoplasma Detection Kit	Lonza	Cat No. LT07-703
Invitrogen Taq polymerase	Thermo Fisher	Cat No. 10342020
Experimental models: Cell lines		
HEK293T	ATCC	ATCC CRL-3216
HC-derived primary dermal fibroblasts	ATCC	Cat No. CRL2088
HC-derived primary dermal fibroblasts	Coriell institute	Cat No. GM03440, GM08447
DS-derived primary dermal fibroblasts	ATCC	Cat No. CCL54
DS-derived primary dermal fibroblasts	Coriell institute	Cat No. AG08942, GM04616
Oligonucleotides		
MX1 mRNA TaqMan FAM Hs200895608_m1	Thermo Fisher	Cat No. 4331182
IFI27 mRNA TaqMan FAM Hs01086373_g1	Thermo Fisher	Cat No. 4351370
IFIT1 mRNA TaqMan FAM Hs03027069_s1	Thermo Fisher	Cat No. 4331182
USP18 mRNA TaqMan FAM Hs00276441_m1	Thermo Fisher	Cat No. 4331182
RSAD2 mRNA TaqMan FAM Hs00369813_m1	Thermo Fisher	Cat No. 4351370
IFNAR2 CRISPR gRNA ATTTCCGGTCCATCTTATCA	IDT	N/A
USP18 CRISPR gRNA CATTACGAACACCTGAATCA	IDT	N/A
Recombinant DNA		
pMET7-IFNAR2	Laboratory of Sandra Pellegrini	N/A
IFNAR2_TETonBFP_TRE3G	This paper	N/A
Reverse Tetracycline-Controlled Transactivator (rtTA)	Addgene	Plasmid No. 66810
pCAGGS-VSV-G	This paper	N/A
pCMV-Gag/Pol	This paper	N/A
Software and algorithms		
Cytobank	Beckman Coulter	N/A
FlowJo	Becton Dickinson Company	N/A
Fiji	ImageJ	N/A
Cell Profiler	Broad Institute	N/A
GraphPad Prism 9	GraphPad Software	N/A

RESOURCE AVAILABILITY

Lead contact

Further information and requests for resources and reagents should be directed to and will be fulfilled by the lead contact, Dusan Bogunovic (dusan.bogunovic@mssm.edu).

Materials availability

All plasmids and cell lines used in this study are available from the lead contact.

Data and code availability

- The data that support the findings of this study are available in the article and supplementary materials.
- This paper does not report original code.
- Any additional information required to reanalyze the data reported in this paper is available from the lead contact upon request.

EXPERIMENTAL MODEL AND SUBJECT DETAILS

Human samples

The study was approved under the IRB protocol at Mount Sinai Health System (MSHS) (IRB-18-00638/ STUDY-18-00627). Patients were approached either in person at the hospital or via email obtained through the NIH's DS-Connect ® national registry (dsconnect.nih.gov). Recruited patients were 60% male, 40% female, 15.3 years mean age (range: 1.5–38 years). All patient data were de-identified. Written informed consent for all individuals in this study was provided in compliance with an institutional review board protocol. All uninfected patient samples were drawn in the context of an outpatient routine visit and patients exhibited no signs of infection (fever, runny nose, cough, sore throat). From each patient, blood was drawn into a Cell Preparation Tube with sodium heparin (BD Vacutainer). PBMCs were isolated from using Ficoll separation and stored at −80°C until use. Whole blood was stimulated or not with cytokine and fixed using Proteomic Stabilizer PROT1 (SmartTube) and frozen at −80°C.

Cell lines

DS- and HC-derived primary dermal fibroblasts were obtained from ATCC (CCL54, CRL2088) and Coriell (AG08942, GM04616, GM03440, GM08447) and immortalized with hTERT (2 male and 1 female line for both HC and DS). Constitutively-expressing USP18 cells were previously generated in the lab (Marta NEJM). hTERT fibroblasts, HEK293Ts, and A549 cells were cultured in DMEM containing 10% fetal bovine serum (FBS) (Invitrogen), 1% GlutaMAX (GIBCO), and 1% penicillin/streptomycin (GIBCO). All cells were cultured at 37°C and 10% CO2. All cell lines were routinely tested for mycoplasma contamination with the MycoAlert PLUS Mycoplasma Detection Kit (Lonza) according to the manufacturer's instructions.

METHOD DETAILS

Cloning

IFNAR2-pMET7 (generously provided by Sandra Pellegrini) was subcloned with In-Fusion (Takara) into a lentiviral compatible vector with a TETon 3G (TRE3G) promoter and BFP expressed from a separate constitutive promoter (generously provided by Ben Tenoever). The TETon system was combined with a separate lentiviral compatible vector containing the reverse tetracycline-controlled transactivator (rtTA) (Addgene: 66810).

Lentiviral particles were generated by co-transfection of TETon-IFNAR2 or rtTA and pCAGGS-VSV-G, pCMV-Gag/Pol by CaCl2 transfection of HEK293Ts. Supernatants were collected 48 h later, purified, and transferred to target cells with polybrene. Cells were selected with Hygromycin (200 μg/mL) and sorted for BFP expression.

CRISPR editing

CRISPR editing was performed with Alt-® S.p. Cas9 Nuclease V3 (IDT 1081058) and Alt-R crRNA guide RNAs (IDT) transfected into hTERTs with a 4D-Nucleofector (Lonza) using the manufacturer's optimized protocol for primary cells (P3 solution). Single-cell clones from CRISPR-generated KOs were isolated via limiting dilution on a feeder layer of irradiated hTERTs. KOs were screened by Flow cytometry and Western blot for the absence of IFNAR2 and USP18 (Figures 1E and S2B) and competence of signaling in response to IFNa2b (Figure S2C).

Targeted gene	Guide sequence
IFNAR2	ATTTCCGGTCCATCTTATCA
USP18	CATTACGAACACCTGAATCA

RNA isolation and quantitative PCR

All cytokine stimulations were performed as indicated with IFN-α 2b (Intron-A) in complete DMEM. RNA was extracted from hTERT-immortalized fibroblasts (Qiagen RNeasy) complete PBMCs (Direct-zol RNA Microprep) and reverse-transcribed (ABI High-Capacity Reverse Transcription). The expression of ISGs (MX1, IFIT1, RSAD2, IFI27, and USP18), relative to the 18S or GAPDH housekeeper gene, was analyzed by TaqMan quantitative real-time PCR (TaqMan Universal Master Mix II with uracil-DNA glycosylases) on a Roche LightCycler 480 II. The relative levels of ISG expression were calculated by the ΔΔCT method, relative to the mean values for the mock-treated controls.

IFNAR negative regulation

To test IFN refractoriness, hTERTs were seeded overnight at 50,000 cells/mL in 12-well plates and stimulated (Primed) or not (Naïve) with 10 IU/mL IFNα2b for 8–16 h, washed 3 times with PBS, and allowed to rest in DMEM for 36 h. For Jak inhibition (Primed + TOFA), cells were treated with overnight IFNα2b and Tofacitinib (50mM) was added to the wells 30 min after the initiation of the treatment. Cells were then washed 3 times with PBS and allowed to rest in DMEM for 36 h. Cells were then re-stimulated with 10 or 100 IU/mL IFNα2b as indicated for 15 min followed by immunoblotting. In the dox-inducible IFNAR2 system, cells were cultured in

DMEM + doxycycline for 48 h before the prime, and the prime and rest were also performed in DMEM + doxycycline. All experiments were performed with n = 3 biological replicates.

Protein assays

Whole-cell extracts for immunoblotting were prepared by incubating cells for 20 min in RIPA lysis buffer (Thermo Fisher Scientific) with 50 mM dithiothreitol and Protease/Phosphatase inhibitor cocktail (Cell Signaling Technology). Protein was quantified with Micro BCA Protein Assay (Thermo Fisher Scientific). Immunoblotting was performed using the Bio-Rad Western blot workflow. Membranes were blocked in 5% BSA for primary antibodies or 5% nonfat dry milk for secondary antibodies. Antibodies used were STAT1 (Santa Cruz Biotechnology), STAT2 (Millipore), phospho-Tyr 701 STAT1 (Cell Signaling Technology), phospho-Tyr 689 STAT2 (Cell Signaling Technology), USP18 (Cell Signaling Technology), IFIT1 (Cell Signaling Technology), MX1 (Abcam), SOCS1 (Thermo Fisher Scientific), β-actin (ABclonal), and GAPDH (Millipore). Signal was detected with enhanced chemiluminescence detection reagent (ECL or SuperSignal West pico, Thermo Fisher Scientific) by film development or capturing on ImageQuant 800 Fluor imaging system (Cytiva). For all representative immunoblots shown, n = 3 separate experiments were carried out.

Flow cytometry

Phospho-STAT1 staining: Whole blood from individuals with DS and HC were subject to Ficoll gradient to collect the mononuclear cell layer (PBMC) and frozen. For direct stimulation, thawed PBMCs were incubated in complete RPMI overnight, washed, stained with live-dead in PBS for 10 min at 37°C, and finally were stimulated for 15 min with indicated amounts of IFNα2b. For staining, cells were washed 2 times with 0.5% BSA and surface-stained on ice for 30 min (CD16-AF647, CD14-AF488, CD3-BV510, CD19-AF700, CD56-BV711, all from Biolegend) followed by fixation/permeabilization in 90% ice-cold methanol and staining with PE anti-phospho-STAT1 Y701 (1:25, BD).

IFNAR1 and IFNAR2 staining: hTERT-immortalized fibroblasts were scraped off in 5mM EDTA, washed, and stained with live-dead in PBS for 30 min on ice. They were then washed and stained with anti-IFNAR1 (clone AA3, courtesy of Sandra Pellegrini in Figure S1A and clone MARI-5A3 from Millipore Sigma for Figure S3A) or anti-IFNAR2 (PBL) for 2 h on ice. The cells were washed and stained with biotin-conjugated rat anti-mouse IgG (H + L) (Thermo Fisher) for 40 min on ice, followed by PE-conjugated Streptavidin for 10 min on ice.

Flow cytometry was acquired on a Cytek Aurora or BD LSR Fortessa, and data were analyzed with Cytobank (https://www.cytobank.org/).

Mass cytometry

Whole blood from the patient and HC were stimulated for 15 min with as indicated with IFN-α2b (Intron-A) in RPMI or mock-treated, fixed using Proteomic Stabilizer PROT1 (SmartTube) and frozen at −80°C. Fixed whole blood was stained and analyzed by mass cytometry (CyTOF) at the Human Immune Monitoring Center of the Icahn School of Medicine at Mt. Sinai. Samples were barcoded then stained together with antibodies against selected surface markers for 30 min on ice. Cells were then washed and fixed, resuspended in diH2O containing EQ Four Element Calibration Beads (Fluidigm), and acquired on a CyTOF2 Mass Cytometer (Fluidigm). Data files were normalized by using a bead-based normalization algorithm (CyTOF software, Fluidigm) and debarcoded using CD45 gating. The gated populations were visualized in lower dimensions using viSNE in Cytobank and manually gated based on the previously described gating scheme (Geanon et al., 2020).

Viral challenges

Influenza A Virus challenge: Cells were exposed to PR8-GFP (Influenza A/PR/8/34 (PR8) virus (H1N1), generously provided by Adolfo Garcia-Sastre) overnight at indicated dilutions from stock. Following the incubation period, cells were fixed and permeabilized with the BD Fixation/Permeabilization kit (BD). Cells were fixed for 20 min at 4°C and stained with DAPI (1:10,000 in 1XPerm/Wash buffer) for 20 min at RT. Cells were then washed and left in PBS. DAPI and GFP signals were acquired on a Celigo Imaging Cytometer (Nexcelom) and quantified in CellProfiler (McQuin et al., 2018). Experiments were carried out with n = 3 biological replicates.

Zika Virus challenge: Cells were exposed to ZIKV (strain PRVABC59, GenBank: KU501215.1) for one hour, washed three times, and allowed to rest overnight. Supernatants from these cells were then harvested and diluted at 1:100 dilution followed by 1:3 serial dilutions and placed on previously plated Veros (ATCC). After 7 days, Veros were fixed and permeabilized with the BD Fixation/Permeabilization kit (BD). Cells were fixed for 20 min at 4°C and stained with anti-Flavivirus Group Antigen 4G2, 1:1000 (Millipore) for 1 h at RT. Cells were then washed and stained with secondary (1:10,000) and DAPI for 45 min at RT. Cells were then washed and DAPI and AF647 signals were acquired on a Celigo Imaging Cytometer (Nexcelom).

Immunity, Volume *55*

Supplemental information

Excessive negative regulation of type I interferon disrupts viral control in individuals with Down syndrome

Louise Malle, Marta Martin-Fernandez, Sofija Buta, Ashley Richardson, Douglas Bush, and Dusan Bogunovic

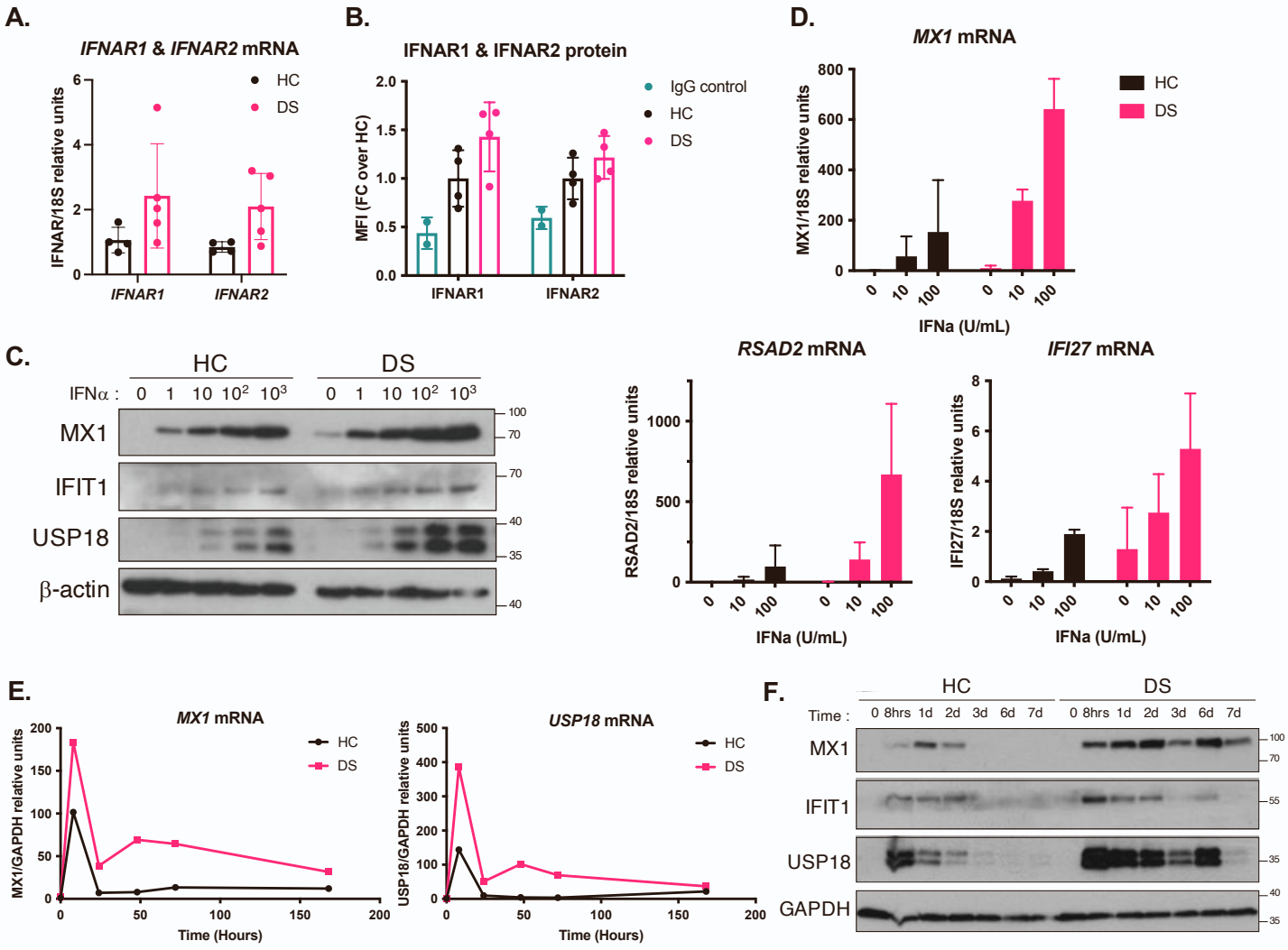

Supplemental Figure 1. Hyper-response to IFN-I in DS hTERT fibroblasts.
(A) qPCR and **(B)** Flow cytometry quantification of *IFNAR1* and *IFNAR2* expression in hTERT-immortalized fibroblasts from healthy controls (HC, *n=4*) or individuals with DS (DS, *n=4*).
(C) Immunoblotting and **(D)** qPCR for ISG induction in HC (*n=4*) and DS (*n=4*) hTERT-immortalized fibroblasts stimulated for 30 min with indicated doses of IFN-α (IU/mL) followed by rest in untreated media for 24 hours (protein, B) or 6 hours (mRNA, C).
(E) qPCR and **(F).** Immunoblotting for ISG induction after stimulation with IFN-α (10 IU/mL) for 8 hours, wash, and rest for indicated times. Result representative of of fibroblasts derived from *n=3* HCs and *n=3* individuals with DS.

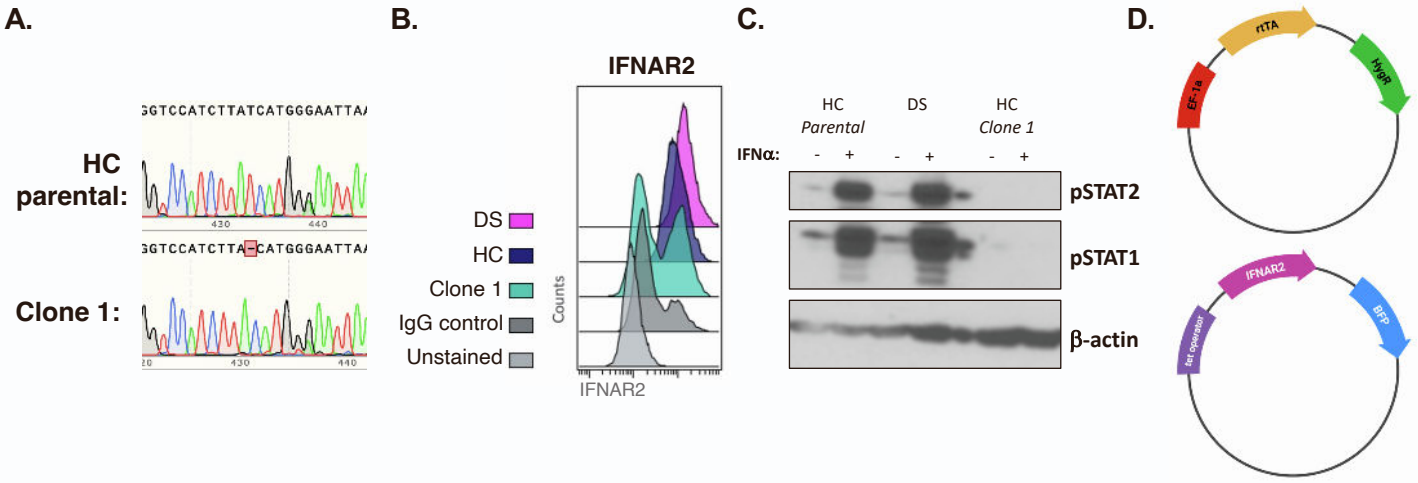

Supplemental Figure 2. Doxycycline-inducible *IFNAR2* system in hTERT fibroblasts.
(A) Sanger sequencing of genomic DNA confirming 1 amino acid deletion in *IFNAR2* knockout Clone 1.
(B) Flow cytometry quantification of *IFNAR2* confirming lack of expression in *IFNAR2* knockout Clone 1.
(C) Immunoblotting for STAT phosphorylation after stimulation for 30 min with IFN-α (1000 IU/mL) confirming lack of response in *IFNAR2* knockout Clone 1.
(D) Diagram of 2-plasmid system used for lentiviral doxycycline-inducible *IFNAR2* expression.

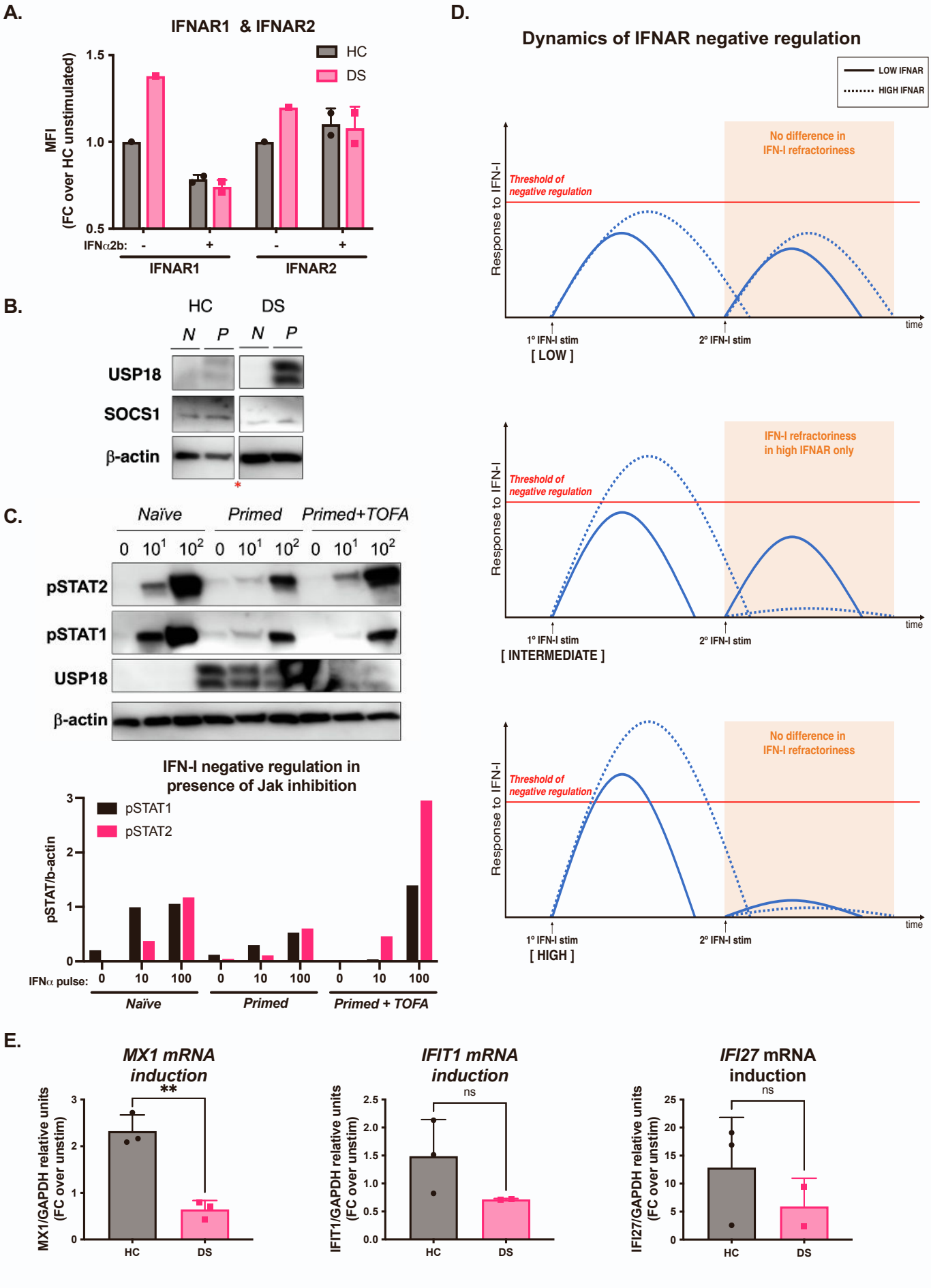
A.
IFNAR1 & IFNAR2
HC
DS
MFI
(FC over HC unstimulated)
1.5
1.0
0.5
IFNα2b: - + - +
IFNAR1
IFNAR2
B.
HC DS
N P N P
USP18
SOCS1
β-actin
*
C.
Naïve Primed Primed+TOFA
0 10¹ 10² 0 10¹ 10² 0 10¹ 10²
pSTAT2
pSTAT1
USP18
β-actin
IFN-I negative regulation in presence of Jak inhibition
pSTAT1
pSTAT2
pSTAT/b-actin
IFNα pulse: 0 10 100 0 10 100 0 10 100
Naïve
Primed
Primed + TOFA
D.
Dynamics of IFNAR negative regulation
LOW IFNAR
HIGH IFNAR
Response to IFN-I
Threshold of negative regulation
No difference in IFN-I refractoriness
time
1° IFN-I stim
2° IFN-I stim
[LOW]
IFN-I refractoriness in high IFNAR only
[INTERMEDIATE]
[HIGH]
E.
MX1 mRNA induction
**
MX1/GAPDH relative units (FC over unstim)
HC
DS
IFIT1 mRNA induction
ns
IFIT1/GAPDH relative units (FC over unstim)
IFI27 mRNA induction
IFI27/GAPDH relative units (FC over unstim)

Supplemental Figure 3. Increased IFNAR negative regulation in Down syndrome.
(A) Flow cytometry quantification of *IFNAR1* and *IFNAR2* expression in the HC and DS hTERT-immortalized fibroblasts previously stimulated (+) or not (+) with a primary stimulus of IFN-α (10 IU/mL) for 12 h, washed, and allowed to rest for 36 h.
(B) Immunoblotting for SOCS1 in HC and DS hTERT-immortalized fibroblasts previously stimulated (N) or not (P) with a primary stimulus of IFN-α (10 IU/mL) for 12 h, washed, and allowed to rest for 36 h. *image was cropped to remove irrelevant lanes.
(C) DS hTERT-immortalized fibroblasts were or untreated (Naïve) or stimulated with IFN-α (10 IU/mL) for 8 hours and Tofacitinib (50mM) was added at hour 2 (Primed +TOFA) or not (Primed). Cells were washed, allowed to rest for 36 h, and re-stimulated for 15 min with IFN-α. Immunoblotted for STAT phosphorylation and quantification.
(D) Diagram of engagement of IFN-I refractoriness with increasing levels of IFN-α priming dose and increasing levels of *IFNAR2* expression.
(E) qPCR for ISG induction in PBMCs derived from HCs (*n=2*) and individuals with DS (*n=3*), stimulated with 100 IU/mL IFN-α for 30 min followed by rest in untreated media for 6 hours (mRNA, C). Expressed as fold-induction over individual's baseline.